NUMERICAL ANALYSIS OF SCATTERING BY INTERFACE FLAWS

Yonglin Xu and Jan D. Achenbach

Center for Quality Engineering and Failure Prevention
Northwestern University
Evanston, IL 60208, USA

INTRODUCTION

Scattering by inhomogeneities in homogeneous media can be analyzed in an elegant manner by reducing the problem statement to the solution of a system of singular integral equations over the surface of the scatterer [1]. This system can be solved in a relatively straight forward manner by the use of the boundary element method [2]. An inhomogeneity in an interface between two solids of different mechanical properties presents some additional complications to the numerical analyst. These complications are discussed in this paper. In deriving the system of singular integral equations, it was decided to use the Green's functions for the unbounded regions of the two materials, rather than the single Green's function for the space of the joined half spaces. This approach introduces a considerable simplification in the integrands, but at the expense of the addition of a set of boundary integral equations over the interface between the two solids, outside of the inhomogeneity. In the boundary element approach the domain of these equations has to be truncated. Specific results are presented for backscattering by a spherical cavity in the interface of solids of different elastic moduli and mass densities.

PROBLEM FORMULATION

The interface of two elastic solids of different mechanical properties, which is defined by $x_3 = 0$, intersects a cavity of arbitrary shape. The origin of the coordinate system is placed in the intersection of the cavity and the interface. The geometry is shown in Fig. 1.

Steady-state time-harmonic fields are considered in this paper.The time harmonic term $\exp(-i\omega t)$,where ω is the angular frequency will,however,be omitted.To distinguish the fields in the upper half-space from those in the lower half-space we use the following notation

$$x_3 < 0: \underset{\sim}{u}(x),\ \underset{\sim}{t}(x),\ c_L,\ c_T; \qquad x_3 > 0: \overline{\underset{\sim}{u}}(x),\ \overline{\underset{\sim}{t}}(x),\ \overline{c}_L,\ \overline{c}_T$$

Here $\underset{\sim}{u}(x)$ and $\underset{\sim}{t}(x)$ define the total displacement and traction fields,while $c_L=\{(\lambda+2\mu)/\rho\}^{1/2}$, $c_T=\{\mu/\rho\}^{1/2}$ are the velocities of longitudinal and transverse waves, respectively.

Review of Progress in Quantitative Nondestructive Evaluation, Vol. 9
Edited by D.O. Thompson and D.E. Chimenti
Plenum Press, New York, 1990

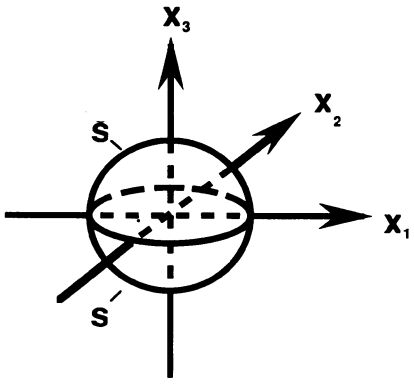

Fig. 1. Cavity in an interface of materials with different machanical Properties.

The surface of the cavity is free of tractions. The surface of the cavity in the upper half-space is denoted by $\bar{S}$, while S denotes the surface of the cavity in the lower half-space. Thus we have

$$\underset{\sim}{x} \in \bar{S}: \ \bar{t}_i = \bar{\tau}_{ij}\, \bar{n}_j = 0 \quad \text{and} \quad \underset{\sim}{x} \in S: \ t_i = \tau_{ij}\, n_j = 0 \tag{1a,b}$$

where τ_{ij} denotes the stress tensor , and $\underset{\sim}{\bar{n}}$ and $\underset{\sim}{n}$ are unit vectors normal to $\bar{S}$ and S, respectively. Tractions and displacements are continuous across the interface outside the cavity, which is denoted by Γ. Thus,

$$\underset{\sim}{x} \in \Gamma: \ \bar{\tau}_{3i} = \tau_{3i}, \quad \bar{u}_i = u_i \tag{2a,b}$$

The incident longitudinal wave in the half-space $x_3 < 0$ is of the general form

$$\underset{\sim}{u}^{in} = A\, \underset{\sim}{d}^{in} \exp(ik_L\, \underset{\sim}{p}^{in} \cdot \underset{\sim}{x}) \tag{3}$$

where

$$\underset{\sim}{d}^{in} = \underset{\sim}{p}^{in} = (\sin\theta^{in}, 0, \cos\theta^{in}) \tag{4a,b}$$

If there were no cavity, the incident wave would give rise to reflected and transmitted longitudinal and transverse waves:

reflected: $$\underset{\sim}{u}^{\alpha} = R^{\alpha} A\ \underset{\sim}{d}^{\alpha} \exp(ik_{\alpha}\ \underset{\sim}{p}^{\alpha} \cdot \underset{\sim}{x}) \tag{5}$$

transmitted: $$\underset{\sim}{\bar{u}}^{\alpha} = T^{\alpha} A\ \underset{\sim}{\bar{d}}^{\alpha} \exp(ik_{\alpha}\ \underset{\sim}{\bar{p}}^{\alpha} \cdot \underset{\sim}{x}) \tag{6}$$

Here α = L for longitudinal waves and α = T for transverse waves. The angle of incidence and the angles of reflection and transmission, as well as the unit vectors $\underset{\sim}{d}$ and $\underset{\sim}{p}$ are shown in Fig.2. The (geometrical) fields are

$$x_3 < 0 : \underset{\sim}{u}^{g}(\underset{\sim}{x}) = \underset{\sim}{u}^{in}(\underset{\sim}{x}) + \underset{\sim}{u}^{L}(\underset{\sim}{x}) + \underset{\sim}{u}^{T}(\underset{\sim}{x}) \tag{7}$$

$$x_3 > 0 : \underset{\sim}{\bar{u}}^{g}(\underset{\sim}{x}) = \underset{\sim}{\bar{u}}^{L}(\underset{\sim}{x}) + \underset{\sim}{\bar{u}}^{T}(\underset{\sim}{x}) \tag{8}$$

The computation of the reflection and transmission coefficients has been discussed elsewhere, see e.g. [3]. Briefly stated, the application of the continuity conditions (2a,b) over the plane $x_3 = 0$ yields relations between the angles θ_α, $\bar{\theta}_\alpha$, and θ^{in} (Snell's law), as well as a set of four linear algebraic equations for R^α and T^α. The latter equations can be solved for R^α and T^α to yield lengthy expressions, which are not reproduced here. For the special case of normal incidence ($\theta^{in} = 0$) we have, however, the simple forms

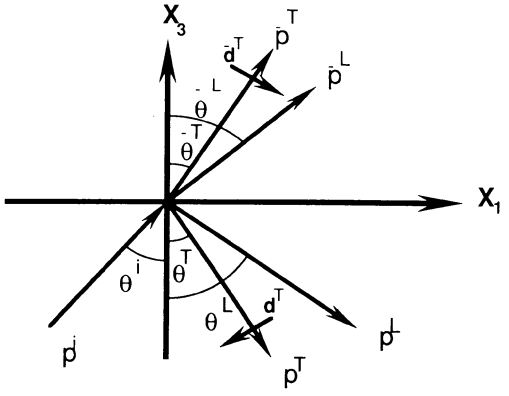

Fig. 2. Propagation vectors of plane waves reflected and transmitted by the interface.

$$R^L = \frac{\bar{\rho}\bar{c}_L - \rho c_L}{\bar{\rho}\bar{c}_L + \rho c_L}, \qquad T^L = \frac{2\,\rho c_L}{\bar{\rho}\bar{c}_L + \rho c_L}, \tag{9a,b}$$

The presence of the cavity perturbs the system of incident, reflected and transmitted fields by the generation of scattered fields $\underset{\sim}{u}^{s}(\underset{\sim}{x})$ and $\underset{\sim}{\bar{u}}^{s}(\underset{\sim}{x})$. Thus, the total fields become

$$x_3 < 0: \; \underset{\sim}{u}(\underset{\sim}{x}) = \underset{\sim}{u}^g(\underset{\sim}{x}) + \underset{\sim}{u}^s(\underset{\sim}{x}); \qquad x_3 > 0: \; \bar{\underset{\sim}{u}}(\underset{\sim}{x}) = \bar{\underset{\sim}{u}}^g(\underset{\sim}{x}) + \bar{\underset{\sim}{u}}^s(\underset{\sim}{x}) \qquad (10a,b)$$

Clearly the scattered field must satisfy the continuity conditions (2a,b) on Γ, while on the surface of the cavity we must have

$$\underset{\sim}{x} \in \bar{S}: \; \bar{\tau}^s_{ij}\, \bar{n}_j = -\bar{\tau}^g_{ij}\, \bar{n}_j \quad \text{and} \quad \underset{\sim}{x} \in S: \; \tau^s_{ij}\, n_j = -\tau^g_{ij}\, n_j \qquad (11a,b)$$

In addition the scattered fields in the two half-spaces must satisfy radiation conditions and regularity conditions as $|\underset{\sim}{x}| \to \infty$.

INTEGRAL REPRESENTATIONS FOR JOINED SOLIDS

The representation of an elastodynamic displacement field in terms of integrals over surfaces bounding a domain, is well known, see e.g. Ref.[4]. In the present problem we will consider four domains: the domain inside the cavity in the lower half-space (V), the lower half-space excluding the domain of the cavity (L-V), the domain inside the cavity in the upper half-space ($\bar{V}$) and the upper half-space excluding the domain of the cavity ($\bar{L}$-$\bar{V}$). For the scattering problem that is being considered in this paper, The scattered displacement field in L-V may then written as

$$C\, u^S_i(\underset{\sim}{x}) = \int_{S+\Gamma_-} [U_{ij}(\underset{\sim}{x},\underset{\sim}{y})\, t^S_j(\underset{\sim}{y}) - T_{ij}(\underset{\sim}{x},\underset{\sim}{y})\, u^S_j(\underset{\sim}{y})]\, dS(y) \qquad (12)$$

where the notation Γ_- indicates that Γ is approached from $x_3 < 0$, and $C = 0$ for $\underset{\sim}{x} \in \bar{L}+V$, $C = 1$ for $\underset{\sim}{x} \in$ L-V and $C = \frac{1}{2}$ for $\underset{\sim}{x} \in S+\Gamma_-$. In Eq.(12), $U_{ij}(\underset{\sim}{x},\underset{\sim}{y})$ is the fundamental solution.

Due to space limitations the detailed derivation of the system of integral equations will be given elsewhere [5]. Here we simply state the following system of equations:

$\underset{\sim}{x} \in S$:

$$\tfrac{1}{2} u_i = -\int_S T_{ij}\, u_j\, dS - \int_{\bar{S}} \bar{T}_{ij}\, \bar{u}_j\, dS + \int_{\Gamma_-} [(U_{ij} - \bar{U}_{ij})\, t_j - (T_{ij} - \bar{T}_{ij})\, u_j]\, dS$$

$$- \int_{\Gamma_-+\Gamma_-^0} [(U_{ij} - \bar{U}_{ij})\, t^g_j - (T_{ij} - \bar{T}_{ij})\, u^g_j]\, dS + u^g_i \qquad (13)$$

$\underset{\sim}{x} \in \bar{S}$:

$$\tfrac{1}{2} \bar{u}_i = -\int_{\bar{S}} \bar{T}_{ij}\, \bar{u}_j\, dS - \int_S T_{ij}\, u_j\, dS + \int_{\Gamma_+} [(\bar{U}_{ij} - U_{ij})\, \bar{t}_j - (\bar{T}_{ij} - T_{ij})\, \bar{u}_j]\, dS$$

$$\int_{\Gamma_+ + \Gamma_+^0} [(\bar{U}_{ij} - U_{ij})\, t_j^g - (\bar{T}_{ij} - T_{ij})\, u_j^g]\, dS + \bar{u}_i^g \qquad (14)$$

$\underset{\sim}{x} \in \Gamma$:

$$\frac{1}{2} u_i = -\int_S T_{ij} u_j\, dS + \int_{\Gamma_-} [U_{ij} t_j - T_{ij} u_j]\, dS - \int_{\Gamma_- + \Gamma_-^0} [U_{ij} t_j^g - T_{ij} u_j^g]\, dS + \frac{1}{2} u_i^g$$

(15)

$$\frac{1}{2} \bar{u}_i = -\int_{\bar{S}} \bar{T}_{ij} \bar{u}_j\, dS + \int_{\Gamma_+} [\bar{U}_{ij} \bar{t}_j - \bar{T}_{ij} \bar{u}_j]\, dS - \int_{\Gamma_+ + \Gamma_+^0} [\bar{U}_{ij} t_j^g - \bar{T}_{ij} u_j^g]\, dS + \frac{1}{2} \bar{u}_i^g$$

(16)

In addition the fields on the interface Γ must satisfy the interface conditions (2a,b).

NUMERICAL RESULTS

For the case that the cavity is a sphere of radius a, solutions of the systems of boundary integral equations have been obtained by the use of the boundary element method. For S and $\bar{S}$ this was achieved by replacing circles in the plane rotating about the x_3 - axis by polygons with 16 ($k_L d < 0.6$) or 20 ($k_L d > 0.6$) sides, as shown in Fig. 3a. Circles in planes normal to the x_3 - axis were maintained as circles, and 12 elements were taken along each circumference. The interface, $\Gamma + \Gamma_0$, is divided into annular elements, as shown in Fig. 3b. The unbounded area Γ was however replaced by a bounded area Γ_b , whose outer boundary was defined by a circle of radius b. For $x_3 = 0, r > b$, $\underset{\sim}{u}^s(0,0,x_3)$ was assumed to be negligible as compared to $\underset{\sim}{u}^g(0,0,x_3)$, In other words the radius r = b was selected such that that the contribution of integrals of the form

$$\int_{\Gamma - \Gamma_b} [(\bar{U}_{ij} - U_{ij})\, t_j^s - (\bar{T}_{ij} - T_{ij})\, u_j^s]\, dS \qquad (17)$$

are negligible. For $k_L d < 0.6$, b/a was taken as b/a = 11, and 12 × 11 elements were used for $\Gamma_b + \Gamma_0$. For $k_L d > 0.6$, b/a =15, and 12 × 15 elements were used for the region. The fields were taken as constants over all elements.

The singular parts of the integrands have been dealt with as described in some detail in Ref.[2]. Thus, the Green's function tractions have been split in singular and nonsingular parts. The singular parts are just the same as the displacements and tractions corresponding to static loading, and they are computed as in the boundary element method for static problems. The dynamic deviations are not singular, and they may be expanded in a series. Usually a small number of terms in the expansions suffice for satisfactory results.

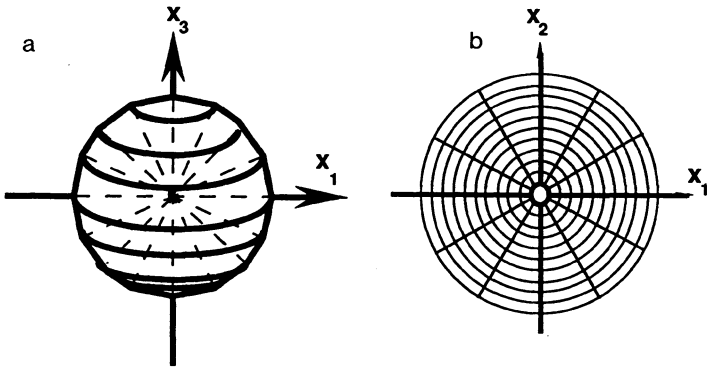

Fig.3(a). Polygon representation of curves rotating about the x_3. (b) Elements in the interface

Specific results have been obtained for an incident wave of the form (3). It should be noted that the system of transmitted waves represented by Eq.(8) does not always consist of a system of homogeneous plane propagating waves. There is a critical angle of incidence, whose magnitude depends on the material properties of the two half-spaces. For incidence of a longitudinal wave at the critical angle the transmitted longitudinal wave grazes the interface, and for incidence beyond the critical angle the transmitted longitudinal wave also propagates along the interface, but with an amplitude which decays with distance to the interface. Details of these phenomena can be found in Refs. [6] and [7]. The method of this paper remains, however, valid, independent of the nature of the transmitted wave.

An interface between two solids of different mechanical properties may give rise to Stoneley waves, i.e., surface waves whose amplitudes decay exponentially with distance from the interface in both materials. Stoneley waves with real-valued wavenumbers occur only within a limited range of material properties of the two materials. A discussion of the existence of Stoneley waves is given in Ref. [8].

Calculations have been carried out for three combinations of the material properties of the two half-spaces. The first case considered concerns materials defined by

$$\nu = 0.29,\ \bar{\nu} = 0.46,\ \bar{\rho}/\rho = 1.19,\ \bar{c}_L/c_L = 1.69$$

For normal incidence and a spherical cavity, the curve marked 2-M of Fig.4 shows the ratio of the amplitudes of the scattered field and the incident wave at the position defined by coordinates (0,0,-16). It is noted that the ratio tends to be quite small, at least at small frequencies. This ratio may be compared with the reflection coefficient given by Eq.(9a) for direct reflection by the interface. The reflection coefficient is R = 0.335. Thus the backscattered wave will be very difficult to distinguish from the reflected field. This observation suggests that a more viable method for detection and characterization of interface voids is by the case of oblique incidence. Oblique incidence was considered for a second combination of material properties:

$$\nu = 0.25,\ \bar{\nu} = 0.23,\ \bar{\rho}/\rho = 0.83,\ \bar{c}_L/c_L = 1.13$$

Figure 5 shows the x_1 and x_3 components of the amplitude ratio of the backscattered field and the incident field for an angle of incidence $\alpha = 30^0$, at the point of observation 20 units removed from the center of the cavity. The backscattered field will now not compete with a specular reflection, and hence more useful results can be extracted from curves of the type shown in Fig.5.

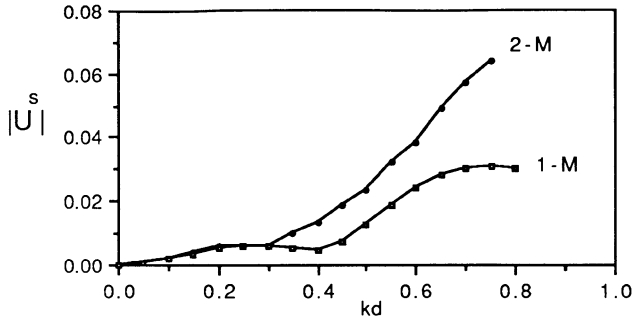

Fig. 4. Absolute values of ratios of amplitudes of the backscattered and the incident fields for two-material case (2-M) and one-material case.

It is also of interest to compare backscattered results for the 2 - material and 1 - material cases, where the 1- material case is the one for the lower half space . For normal incidence, a comparison is included in Fig.4. For a third combination of material properties

$$\nu = 0.25,\ \bar{\nu} = 0.25,\ \bar{\rho} / \rho = 0.8,\ \bar{c}_L/c_L = 1.25,$$

results are shown in Fig.6. It is noted that significant differences due to the presence of the interface occure only at higher frequencies. The difference are very small for Fig.6, because the two materials have the same mechanical impedance, and the reflection coefficient defined by Eq.(9a) actually equals zero.

ACKNOWLEDGMENT

This work was carried out in the course of research sponsored by the Office of Naval Research under Grant No. N00014 - 89 - J -1362 to Northwestern University.

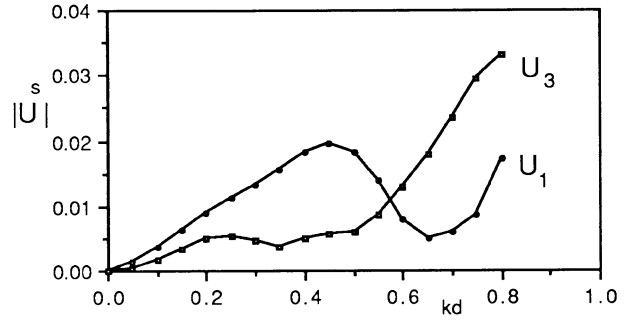

Fig. 5. Amplitude ratios of backscattered displacements in x1 and x3 directions for oblique incidence

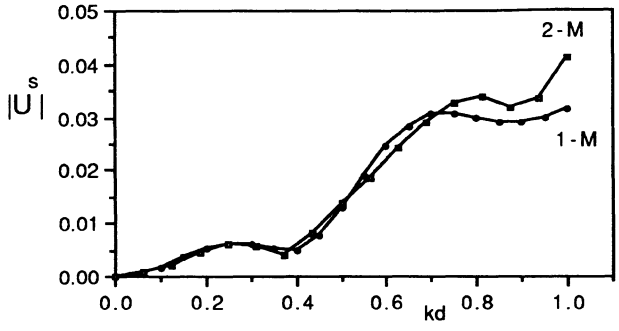

Fig. 6. Ratios of amplitudes of the backscattered and the incident fields for two-material case (2-M) and one material case(1-M).

REFERENCES

1. J.D. Achenbach and M. Kitahara, J. Acoust Soc. Am. 80, 1209 (1986)
2. M. Kitahara and K.Nakagawa, in Boundary Elements VII, edited by C.A. Brebbia and G.Maier, (Springer- Verlag, New York,1985)
3. J.D. Achenbach, Wave Propagation in Elastic Solids , pp.186, (North-Holland Publishing Company, New York,1973)
4. J.D. Achenbach and M. Kitahara, J. Acoust Soc. Am. 81, 595 (1987).
5. Yonglin Xu, Ph.D. dissertation, Northwestern University,1989 (unpublished).
6. I.A. Viktorov, Rayleigh and Lamb Waves (Plenum Press, New York, 1967)
7. Lord Rayleigh, Proc. London Math. Soc. 17, 4 (1885)
8. L.Cagniard, Reflection and Refraction of Progressive Seismic Waves (McGraw-Hill, New York, 1962)